

NOTICE

**CERTAIN DATA
CONTAINED IN THIS
DOCUMENT MAY BE
DIFFICULT TO READ
IN MICROFICHE
PRODUCTS.**

EROSION AND REDEPOSITION OF DIVERTOR AND WALL MATERIALS DURING ABNORMAL EVENTS

A. Hassanein
 Argonne National Laboratory
 9700 S. Cass Avenue, Bldg. 205
 Argonne, IL 60439 USA
 (708) 972-5889

ABSTRACT

High energy deposition to in-vessel components of fusion reactors is expected to occur during abnormal operating conditions. This high energy dump in short times may result in very high surface temperatures which may cause severe erosion as a result of melting and vaporization of these components. One abnormal operating condition results from plasma disruptions where the plasma loses confinement and dumps its energy on reactor components. Another abnormal condition occurs when a neutral beam used in heating the plasma shines through the vacuum vessel to parts of the wall with no plasma present in the chamber. A third abnormal event that results in high energy deposition is caused by the runaway electrons to chamber components following a disruption. The failure of these components under the expected high heat loads can severely limit the operation of the fusion device. The redeposition of the eroded materials from these abnormal events over the first wall and other components may cause additional problems. Such problems are associated with tritium accumulation in the freshly deposited materials, charge exchange sputtering and additional impurity sources, and material compatibility issues.

I. INTRODUCTION

Very high heat fluxes on the plasma chamber wall, on limiters/divertor plates and on other components of a fusion reactor are expected during abnormal operations of fusion devices. One of the abnormal operating conditions may result from plasma disruptions due to plasma instabilities. During a disruption the plasma loses confinement and deposits its energy in very short times on various reactor components such as the divertor plate and parts of the first wall. The exact cause of these instabilities and methods to prevent their occurrence are relatively unknown at

* Work supported by Office of Fusion Energy, U.S. Department of Energy under Contract No. W-31-109-Eng-38.

this time. It is then expected that the next generation of large tokamaks have to be designed to withstand several hundreds of these disruptions. Another abnormal condition results when a neutral beam used in heating the plasma shines through the vacuum chamber to parts of the wall with no plasma present. A third abnormal event results from the generation of runaway electrons with very high energy and their deposition on wall areas following a plasma disruption.

The high energy deposition in short times during various abnormal events will result in very high surface temperatures and may cause melting and vaporization of these components. The net erosion rates resulting from both melting and vaporization are very important in estimating the lifetime of such components.¹ Materials for plasma facing components must have the ability to withstand repeated high heat loads associated with these abnormalities without suffering disabling damage. The effect of plasma disruption on divertor candidate materials for current disruption parameters expected in a machine like ITER is analyzed. The damage expected from a neutral beam shine through to parts of the first wall is also analyzed. The interaction of runaway electrons with reactor components and the resulting damage is discussed elsewhere.²

The redeposition of the eroded material from the divertor plate to the first wall and other component due to a plasma disruption is modeled and analyzed. The growth of these components as a result of the redeposition from a specific disruption event depends mainly on the amount eroded from the divertor plate as well as on geometrical factors of distance and orientation relative to the disruption location on the divertor plate. The spatial distribution and the build up of the redeposited materials are calculated at several locations on the wall. This build up is very important from several viewpoints such as the tritium inventory in these freshly redeposited surfaces, charge exchange sputtering erosion and additional impurity sources, and

material compatibility issues resulting from moving materials from one place to another.

II. DIVERTOR DISRUPTION ANALYSIS

The surface of the divertor plate is subject to repeated vaporization losses because of the high energy deposited on the surface during every plasma disruption. The primary disruption parameters that determine the severity of a disruption event are the energy deposited per unit area, i.e., the energy density, the duration of this deposition, i.e., the disruption time, and the frequency of disruptions or the total number of the expected disruptions during the lifetime of the reactor. The energy density expected on the divertor plate in a device like ITER is around 10-20 MJ/m². The disruption time during the thermal quench has a range from 0.1 to 3 ms, with 0.1 ms believed to be a more realistic value. The total number of disruptions in the ITER physics phase is assumed to be about 500 full load disruptions. In the ITER technology phase the total number of disruptions is about 200. The analysis is done for three potential divertor materials i.e., graphite tiles (carbon-fiber-composites) for the physics phase and tungsten or beryllium coatings for the technology phase. The details of the models used in the calculations are described elsewhere.^{3,4} Prior to the plasma disruption a stationary heat load of about 10 MW/m² is assumed on the divertor plate. Figure 1 shows the vaporized thickness in one disruption at 0.1 ms disruption time for the three candidate materials. The graphite erosion shown in Figure 1 is five times of that predicted by theoretical calculations. This is done to implement the results of recent experimental data on graphite erosion. These experiments showed that the graphite erosion is usually about a factor of five higher than theoretical results under similar conditions. Because of that, graphite erosion is much higher than both tungsten and beryllium. Tungsten vaporization is usually lower than that for beryllium. However, tungsten melting thickness is much larger than beryllium especially at longer disruption times as shown in Figure 2. Vapor shielding is expected to reduce the predicted erosion from vaporization at least by a factor of 2 at these high energy densities.³ Other models may indicate greater protection from vapor shielding.⁵ That may help prolong the divertor lifetime against disruptions. In addition, the melt layer formed during a disruption will be exposed to various forces that may trigger hydrodynamic instabilities within the liquid metal which can lead to the loss of all or part of the melt layer.⁶

If the divertor plate metal coating proposed for the technology phase can be easily

replenished by spraying or by other techniques inside the reactor cavity as the current technology indicates, losses from these severe plasma disruptions can then be tolerated without having to replace the divertor every few disruptions. However, this may not be the case for ITER physics phase where carbon fiber composite is used as a divertor plate material. If the tiles cannot be easily in situ repaired or replaced, the reactor operation may have to be interrupted several times a year to replace the damaged divertor tiles.

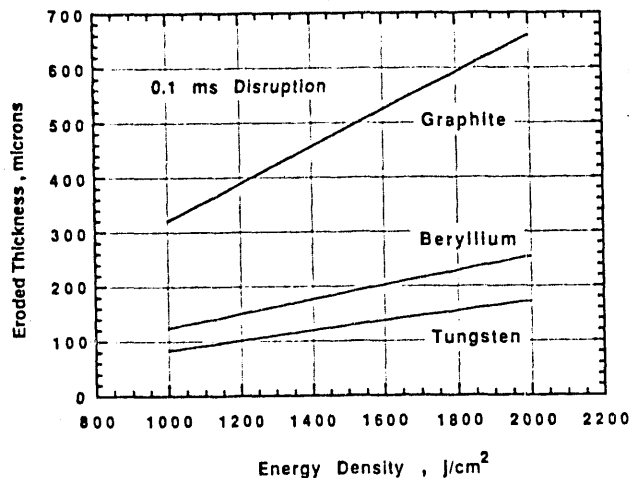


Figure 1. Disruption erosion losses as a function of energy density.

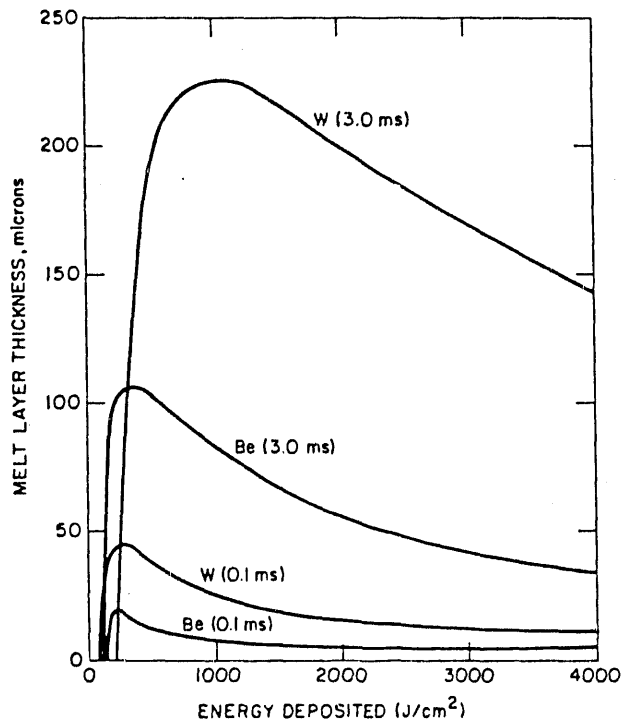


Figure 2. Melt layer thickness for different disruption time.

III. NEUTRAL BEAM DUMP ON THE WALL

This section examines the response of wall areas as a result of neutral beam shine through in the vacuum chamber and then deposit its energy at the wall. This may occur as in the case following a disruption. This problem may be preventable by a proper and an accurate design in which the beam can be turned off very fast. However, the analysis is done to investigate the effect of an accidental beam shine through for periods of time in the order of a few seconds. The beam deposition can either occur at the walls of the reactor or at the surface of the beam gate valve. In either case this may cause serious damage to these components and thus delay or interrupt the operation of the reactor. For this analysis the beam power is only assumed deposited at the surface of the reactor first wall. A typical beam power of about 100 MW in a machine like ITER during a shine through will be deposited on certain spots of the outboard wall facing the beam ports. Assuming three ports each of about 3.4×0.8 m size, a nominal energy flux of about 25 MW/m^2 is expected. An additional peaking factor of 2 can be present, allowing energy fluxes up to 50 MW/m^2 to be deposited on locations at the outboard wall. The response of the wall areas subject to the beam deposition is calculated using an enhanced version of the A*THERMAL-2 computer code.⁴ The analysis is done parametrically with beam energy flux up to 50 MW/m^2 and for deposition times up to 10 seconds. The actual time of deposition depends on how quickly the shine through is discovered and the beam is turned off. The analysis included a radiatively cooled graphite wall (as proposed in ITER physics phase) and a metal coating of tungsten or beryllium on stainless steel structure (as proposed for ITER technology phase). Figure 3 shows the erosion losses from vaporization as a function of the power deposited for both a radiatively cooled graphite wall and the metal coating materials, i.e., tungsten and beryllium. Again, experimental data for carbon erosion losses from vaporization have shown that the actual erosion losses are about five times that of the theoretical predictions. This is shown by the dashed curve in Fig. 3. This makes the graphite wall the least resistant to accidental beam dump compared to metal coating materials. Even without the factor of five, the graphite wall is still worse than beryllium in terms of eroded thickness. This is because of the high operating temperature of the graphite wall. As an example of how serious this problem can be consider the case of 50 MW/m^2 beam power deposited for 10 seconds. The erosion losses can exceed the entire 1 cm tile thickness in just one accident. Tungsten is far more resistant to erosion and melting than beryllium under the same conditions as shown in Figs. 4 and 5. However, shorter deposition

times (i.e., < 1 second), can probably be tolerated for these ranges of beam energy fluxes. Deposition time depends mainly on methods of detection and diagnostic instruments for the neutral beam along with other design factors.

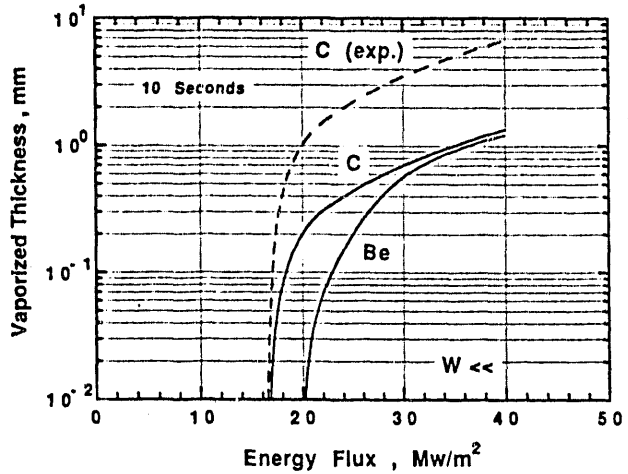


Figure 3. Erosion losses from vaporization for different materials.

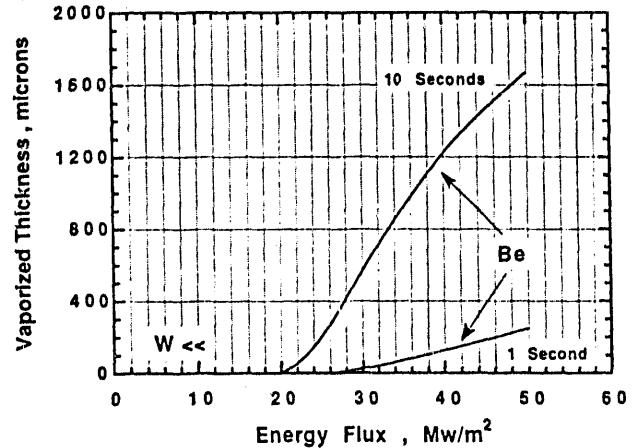


Figure 4. Tungsten and beryllium erosion losses for different energy fluxes.

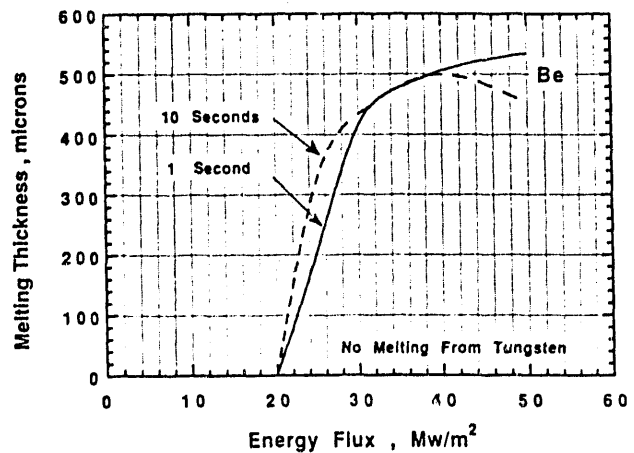


Figure 5. Melting thickness as a function of energy flux and deposition time.

IV. REDEPOSITION OF ERODED MATERIALS

The redeposition of the eroded material from the divertor plate to the first wall as a result of a plasma disruption is analyzed. The amount of the redeposited material from disruption at different locations on the wall depends primarily on geometrical factors of distance from the source (disruption spot on the divertor) to the substrate (i.e., the wall area) and to its orientation relative to the source.

The source of the evaporant material on the divertor plate is simply modeled as a toroidal strip source. This should be a good approximation since the size of the disruption area on the divertor is estimated to be on the order of 20-30 cm wide. This is still very small compared to the dimension of the cavity and wall area. The deposition at different locations is modeled as parallel strips to the toroidal source. The following results from the current model and calculations assume no scattering or interaction between the evaporated material and the plasma particles. This assumption is more likely to over-estimate the growth of the redeposited material on the wall as discussed later on. In addition to the distance between the source and the deposition spot, the orientation of the wall surfaces

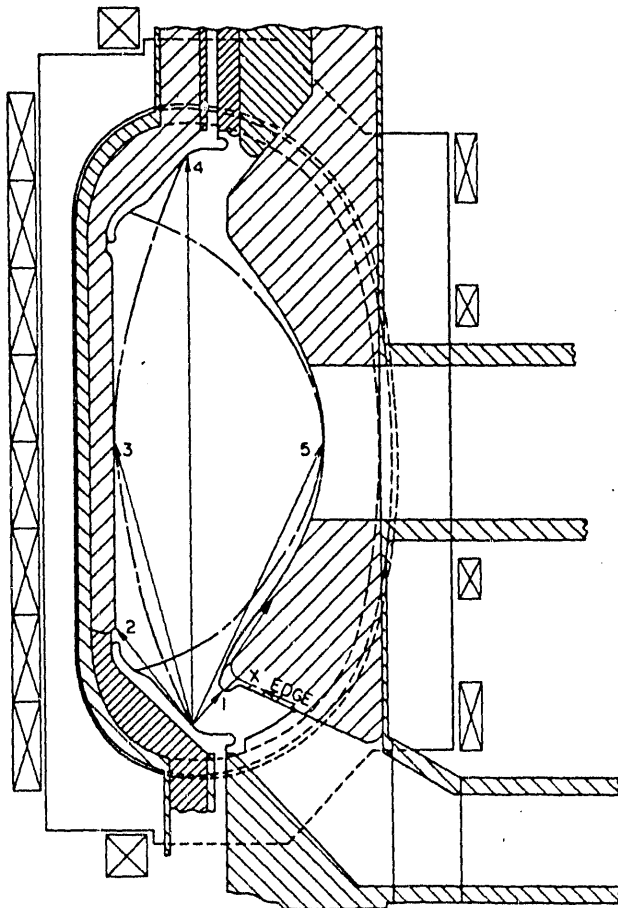


Figure 6. Schematic illustration of reactor cavity and divertor disruption spot.

relative to the direction normal to the source also contributes significantly to the deposition thickness.

Figure 6 shows a schematic illustration of the reactor cavity and different locations on the wall (relative to the disruption spot) where the deposition rates are calculated and compared. Figure 7 shows the predicted deposition thickness at the corresponding locations as a result of 20 MJ/m^2 single disruption at different disruption times. Location 1 is expected to have the maximum deposition thickness not only because it is the closest position to the disruption spot but it is also directly oriented towards it. Longer disruption times do not significantly reduce the erosion or the redeposition at these high disruption energy densities. For the hundreds of disruptions expected, the maximum deposition thickness at or near location 1 could approach the centimeter range. Figure 8 shows a comparison of the deposition thickness profile in wall areas near the divertor plate for different divertor materials. The deposition thickness is calculated for a single disruption at 20 MJ/m^2 and 0.1 ms disruption time. The main difference in the deposition thickness among these materials is due to the amount eroded at the divertor plate during the disruption. The vaporized material from the divertor plate may interact with the incoming plasma ions during the course of the disruption event. This can act as a shielding mechanism for the divertor plate from the plasma ions which results in lower erosion rates.³ Consequently this will reduce the thickness of the redeposited materials. Using the vapor shielding model discussed in reference (3), Figure 9 shows the graphite redeposition thickness on the wall with and without the effect of vapor shielding. The redeposition thickness can be reduced by a factor of two or even more. Comprehensive models need to be developed to

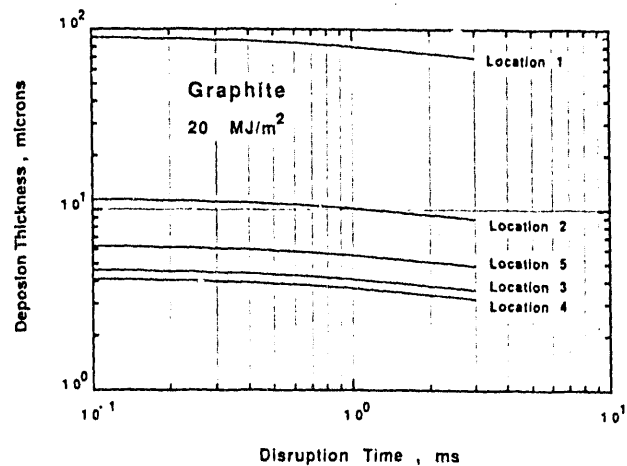


Figure 7. Deposition thickness for various locations on the wall from a divertor disruption.

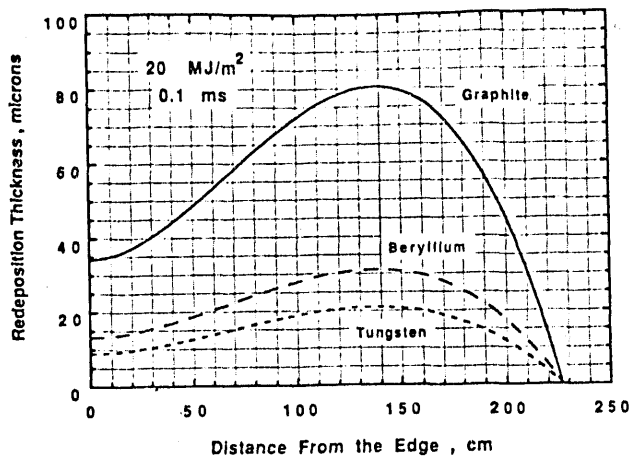


Figure 8. Spatial distribution of redeposited materials on the wall near the divertor plate.

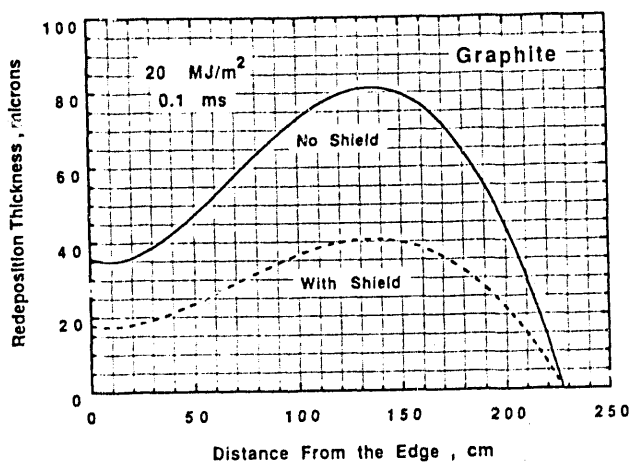


Fig. 9. Redeposition thickness for the graphite divertor with and without vapor shielding effect.

accurately estimate the vapor shielding effect. The deposition profile on the wall along with the surface temperature distribution are very important factors in determining the form of the material deposited, especially for graphite, as well as the tritium inventory accumulated in the redeposited surfaces. Redeposition can also result in additional impurity sources to the plasma during operation.

V. CONCLUSION

Erosion from high energy deposition to in-vessel components of fusion reactors during abnormal events is analyzed. Abnormal events such as plasma disruptions, runaway electrons, and neutral beam shine through the plasma to the walls can cause severe erosion and melting

of reactor components. These high erosion rates can severely limit the operation and the lifetime of fusion devices. Among the potential candidate materials for the plasma facing components, tungsten is the most resistant to erosion during various abnormal operating conditions. The redeposition of the eroded material over the wall, and other components is modeled and analyzed. Several problems may result from such redeposition. Of particular concerns are the tritium accumulation in the freshly deposited surfaces, additional impurity sources due to charge exchange sputtering, and material compatibility issues resulting from transferring different materials from one position to another. Accurate models and analysis are required to further assess the impact of these problems on the performance of the reactor.

REFERENCES

1. A. HASSANEIN, "Response of Materials to High Heat Fluxes During Operation in Fusion Reactors," ASME, 88-WA/NE-2 (1988).
2. K.A. NEIMER et al., "Computational and Experimental Modeling of Runaway Electron Damage," SAND89-2304 (June 1990).
3. A. HASSANEIN et al., Nucl. Engr. Design/ Fusion 1 (3) (1984) 307.
4. A. HASSANEIN, "Modeling the Interaction of High Power Ion or Electron Beams with Solid Target Materials," Argonne National Laboratory Report ANL/FPP/TM-179 (1983).
5. J. GILLIGAN et al., J. Nucl. Mater. 162 (1989) 957.
6. A. HASSANEIN, Fusion Technol. 15 (1989) 513-521.

DISCLAIMER

This report was prepared as an account of work sponsored by an agency of the United States Government. Neither the United States Government nor any agency thereof, nor any of their employees, makes any warranty, express or implied, or assumes any legal liability or responsibility for the accuracy, completeness, or usefulness of any information, apparatus, product, or process disclosed, or represents that its use would not infringe privately owned rights. Reference herein to any specific commercial product, process, or service by trade name, trademark, manufacturer, or otherwise does not necessarily constitute or imply its endorsement, recommendation, or favoring by the United States Government or any agency thereof. The views and opinions of authors expressed herein do not necessarily state or reflect those of the United States Government or any agency thereof.

END

DATE FILMED

06 / 10 / 91

